Available online at www.sciencedirect.com
SCIENCE DIRECT®
Catalysis Today 91–92 (2004) 185–189
CATALYSIS TODAY
www.elsevier.com/locate/cattod

In situ X-ray diffraction studies of the crystallization of $VOHPO_4{\cdot}0.5H_2O$

L. O'Mahony [a,b], D. Sutton [a], B.K. Hodnett [a,b,*]

[a] *Department of Chemical and Environmental Sciences, Materials and Surface Science Institute, University of Limerick, Limerick, Ireland*
[b] *Department of Chemical and Environmental Sciences, University of Limerick, Limerick, Ireland*

Abstract

Time resolved in situ X-ray diffraction was used to study the formation of vanadyl hydrogen phosphate hemihydrate ($VOHPO_4{\cdot}0.5H_2O$) in organic media. This technique has identified a new phase at early synthesis times (less than 300 s) at a *d*-spacing of 7.5 and 3.1 Å. The feature at 7.5 Å shifted to 6.7 Å during the first 20 min of synthesis and this phase collapsed as $VOHPO_4{\cdot}0.5H_2O$ formed. Thin symmetrical platelets of 10 μm × 10 μm dimensions were observed when samples were recovered after short synthesis times. Energy dispersive X-ray analysis indicated that these platelets contained vanadium and phosphorus. The platelets appeared to delaminate possibly associated with the strain generated when the *d*-spacing shifted from 7.5 to 6.7 Å, from which growth of the $VOHPO_4{\cdot}0.5H_2O$ into the familiar rosette morphology occurs.

Keywords: In situ X-ray diffraction; Crystallization; VPO

1. Introduction

The vanadium phosphorus oxide (VPO) catalysts used for *n*-butane oxidation to maleic anhydride are largely composed of $(VO)_2P_2O_7$ which presents a twisted platelet habit of varying crystallinity and featuring small amounts of V^{5+} phases, most notably α-$VOPO_4$ [1,2]. The predominant exposed plane is the basal plane of $(VO)_2P_2O_7$, indexed as the (2 0 0) [3–6]. Evidence has been presented that the yield of maleic anhydride improves when exposure of the (2 0 0) plane of $(VO)_2P_2O_7$ is maximised [7], leading to the proposal that the active site for *n*-butane activation and oxy-functionalisation resides on this plane [8]. Some researchers have emphasised the role of platelet twisting in tuning the surface acid–base properties of VPO catalysts [9,10].

However, the origin of the $(VO)_2P_2O_7$ morphology has not been established. It is related topotactically to the precursor phase, namely $VOHPO_4{\cdot}0.5H_2O$, which presents a near identical morphology to the fully developed catalyst [11,12]. This phase in turn develops when ortho-H_3PO_4 is added to a solution/suspension in which V_2O_5 is partially reduced and dissolved by refluxing in an alcohol, most often isobutanol, or a mixture of isobutanol and benzyl alcohol [4,7]. The hemihydrate phase forms rapidly at reflux when ortho-H_3PO_4 in the appropriate amount is added and the final precursor phase is free of any traces of unreacted V_2O_5 [13].

Preparation methods for the VPO catalysts have been developed empirically, with differing reducing agents and solvents employed to give catalysts of variable efficiencies [14]. In this report we describe an in situ X-ray diffraction study of the evolution of phases during the synthesis of $VOHPO_4{\cdot}0.5H_2O$ combined with ex situ studies wherein the normal preparation method is stopped after extremely short synthesis times. The resulting solid product present in the reaction mixture was analysed by microscopy and ex situ X-ray diffraction. The aim of this study was to establish the mechanism whereby the crystalline phase; $VOHPO_4{\cdot}0.5H_2O$ nucleates and grows into the familiar rosette like morphology.

2. Experimental

V_2O_5 (Merck) was refluxed in a 90:10 alcohol mixture of 2-methyl propan-1-ol (BDH Analar) and benzyl alcohol (Riedel-de Haen) for 4 h. The 85% H_3PO_4 was added to

* Corresponding author. Tel.: +353-61-202246; fax: +353-61-202568.
E-mail address: kieran.hodnett@ul.ie (B.K. Hodnett).

0920-5861/$ – see front matter © 2004 Elsevier B.V. All rights reserved.
doi:10.1016/j.cattod.2004.03.031

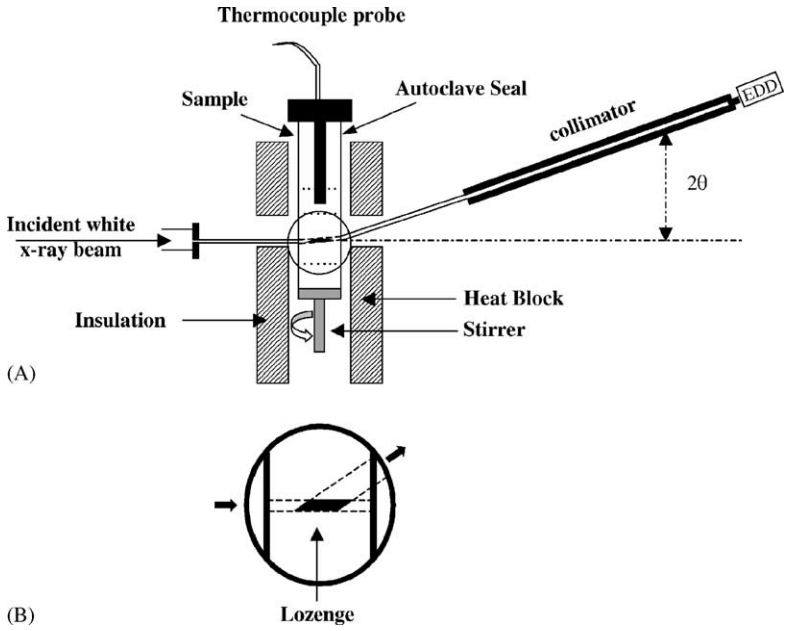

Fig. 1. Schematic representation of in situ energy dispersive diffraction using a white beam synchrotron source.

this suspension keeping the *P*:*V* ratio = 1:1 before transferring to a Teflon lined stainless steel cell under constant stirring. The temperature of the sample under study was automatically controlled and measured using a thermocouple directly inserted into the sample cell. The evolution of crystalline phases with time were then recorded in situ, using an energy dispersive X-ray diffraction set-up at Station 16.4 of the UK Synchrotron Radiation Source (SRS) at the CLRC Daresbury Laboratory, UK. Station 16.4 is a white beam facility that utilises a EDD system that has been designed to considerably increase the overall working *d*-spacing range without compromising the choice of 2θ angle or X-ray apertures [15–18]. This system contains a multi-detector system, which collects XRD patterns from a sample simultaneously at different angles allowing patterns in the regions of 2–5 and 4–15 Å to be generated. A schematic of the in situ X-ray diffraction set-up is presented in Fig. 1.

This study was complimented by ex situ work in which samples of solids from the refluxing vanadium oxide/alcohol/ortho-H_3PO_4 medium were isolated by filtration for times that varied between 0.5 and 240 min. Samples so isolated were also analysed by ex situ X-ray diffraction.

A Focused Ion Beam microscope FEI 200 was used to obtain precursor images. Samples were coated with gold in an Edwards S150B sputter coater. The gallium ion (Ga^+) beam energy is typically 30 keV, with a beam current in the range of 1–11,500 pA.

3. Results and discussion

Figs. 2 and 3 present the in situ diffraction patterns of the VPO phases that develop when phosphoric acid was added

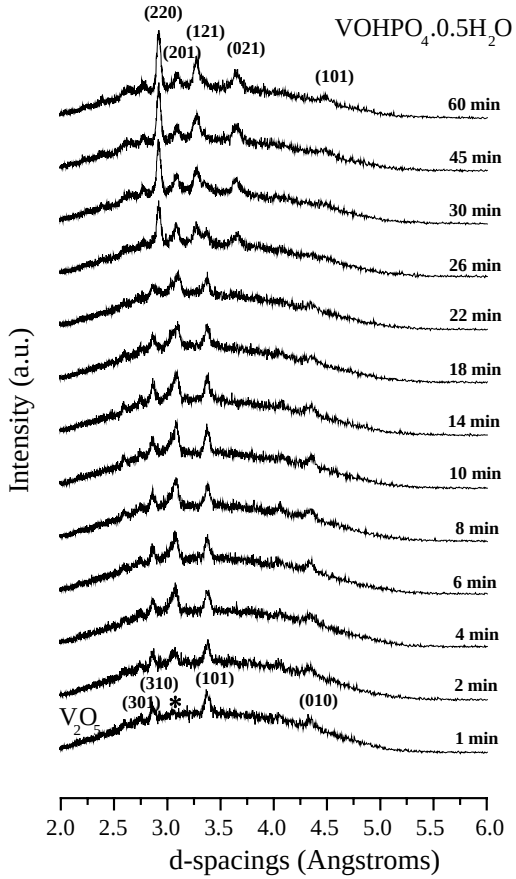

Fig. 2. In situ energy dispersive XRD patterns of $VOHPO_4{\cdot}0.5H_2O$ evolution from V_2O_5 at 115 °C with a reactant *P*:*V* molar ratio of 1:1.

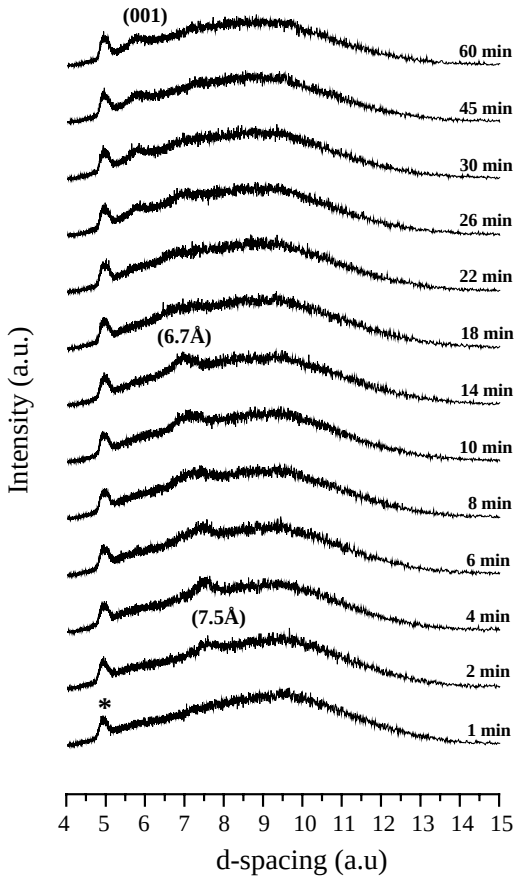

Fig. 3. In situ energy dispersive XRD patterns of $VOHPO_4{\cdot}0.5H_2O$ evolution from V_2O_5 at 115 °C with a reactant *P*:*V* molar ratio of 1:1 (* represents Teflon reflection at 4.9 Å).

to a V^{4+}/VO_x suspension in organic media. A reflection at 4.91 Å is observed in all patterns and is related to Teflon from the lining of the sample cell. Fig. 2 presents the XRD patterns recorded for *d*-spacings in the range 2–5 Å. At short synthesis times the reflections are primarily those of V_2O_5. With increasing reaction time, characteristic phases of V_2O_5 disappear resulting in the formation of the hemihydrate precursor phase. The (1 0 1) and (3 1 0) reflections of V_2O_5 disappear after 18–22 min of reaction. By this time the (1 0 1), (1 2 1) and (2 2 0) reflection of $VOHPO_4{\cdot}0.5H_2O$ begins to form. A consistent feature of this data is the emergence of a peak at 3.1 Å, not present at 1 min, but a major feature in the diffraction pattern after 4 min. This feature was consistently present until ca. 26 min, reduced somewhat in intensity, and re-emerged as the hemihydrate formed fully, at which time it was indexed as the (2 0 1) reflection of $VOHPO_4{\cdot}0.5H_2O$.

Fig. 3 presents the patterns recorded at *d*-spacings 4–15 Å. The patterns show a new peak at 7.5 Å, which forms after just 2 min of reaction but shifts to ca. 6.7 Å after 18 min. By this time, the (0 0 1) phase of the hemihydrate precursor evolves at 5.7 Å with a maximum intensity at 60 min.

The patterns presented in Figs. 2 and 3 are a representative example of a series of experiments in which reaction temperature after the addition of ortho-H_3PO_4, reactant *P*:*V* ratio during preparation and residual undissolved vanadium oxide content of the suspensions were systematically followed using the in situ diffraction technique. Ex situ diffraction techniques did not consistently detect the reflection at 7.5 and 6.7 Å. All other features were detected using ex situ methods.

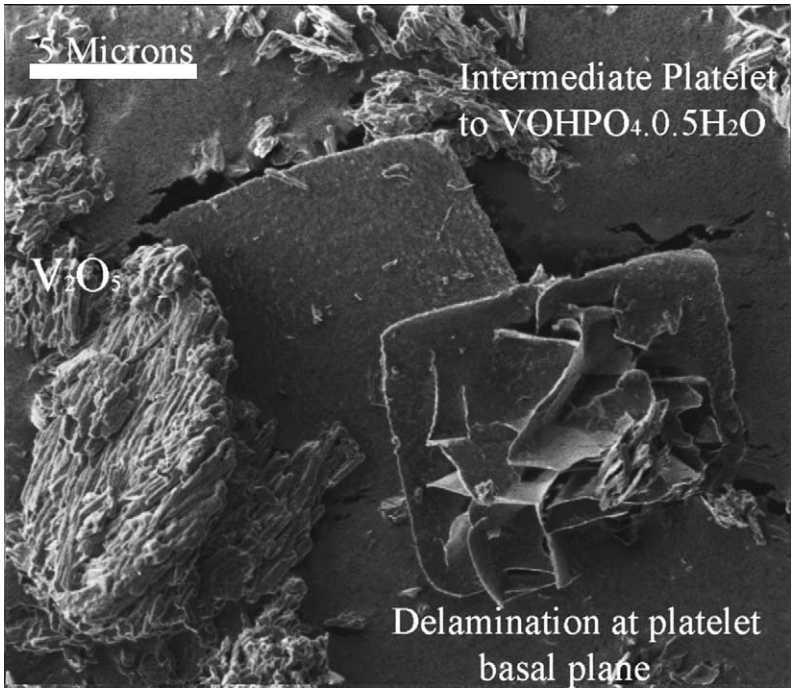

Fig. 4. FIB image of sample recovered after 1.5 min of reaction.

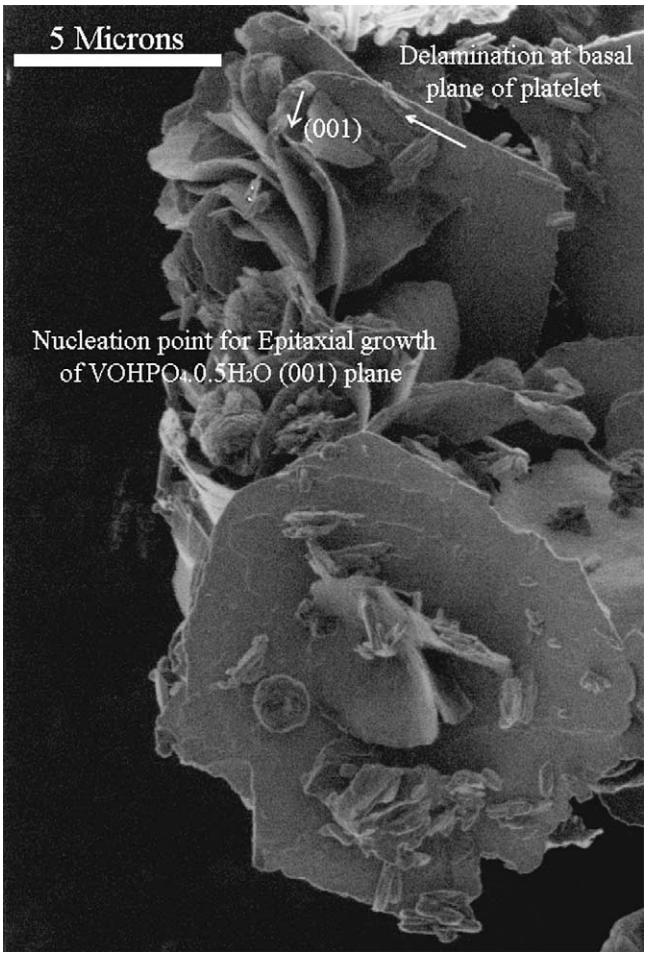

Fig. 5. FIB image of sample recovered after 2 min of reaction.

Figs. 4 and 5 present microscopy (Focused Ion Beam) of the samples recovered at short reaction times in the crystallisation process. Unreacted VO_x is clearly seen in Fig. 4 as well as flat thin platelets (10 μm × 10 μm). EDXA analysis of these platelets indicated that they contain vanadium and phosphorus. However, ex situ XRD analysis indicates that $VOHPO_4{\cdot}0.5H_2O$ is not present at this time in the synthesis. As the synthesis proceeds, these platelets disappear from the micrographs as the familiar rosette type particles of $VOHPO_4{\cdot}0.5H_2O$ emerge. For short synthesis times there was evidence (see Fig. 4) that the thin platelets delaminate, sometimes at the edges and sometimes at the centre of platelets, resulting in short well defined features pointing upwards from the original platelets at various angles. This is the origin of the growth of the $VOHPO_4{\cdot}0.5H_2O$ phase, which is seen at a further, although not fully developed stage in Fig. 5.

In this work we associate the reflections observed in situ at 7.5–6.7 and 3.1 Å, with the platelets observed by microscopy and these phases are identified as $VOPO_4{\cdot}2H_2O$ which partially dehydrates to $VOPO_4{\cdot}H_2O$ [19–21]. These platelets were never observed prior to the addition of phosphorus (ortho-H_3PO_4). Another key feature of this work is the observation that there is some element of delamination, possibly triggered as a mechanism whereby strain is released as the *d*-spacing changes from 7.5 Å ((0 0 1) of $VOPO_4{\cdot}2H_2O$) initially to a value of ca. 6.7 Å ((0 0 1) of $VOPO_4{\cdot}H_2O$) after a synthesis time ca. 20 min. This shift from 7.5 Å to lower *d*-spacings has been observed for all reactions in which the reactant *P*:*V* ratio and synthesis temperature was varied, and this dehydration appears to generate strain within the platelets leading to their delamination, at the edges or centres of the platelets.

Here we hypothesise that the new edges generated on delamination of the platelets act as the nucleation point at which V^{5+} becomes reduced to V^{4+} and from which $VOHPO_4{\cdot}0.5H_2O$ grows inwards and outwards into its familiar rosette like morphology. Two crystallographic features are important in this development, namely the reflection at 7.5–6.7 and 3.1 Å in the platelets and the (0 0 1) (d = 5.7 Å) and (2 0 1) (d = 3.1 Å) reflections in

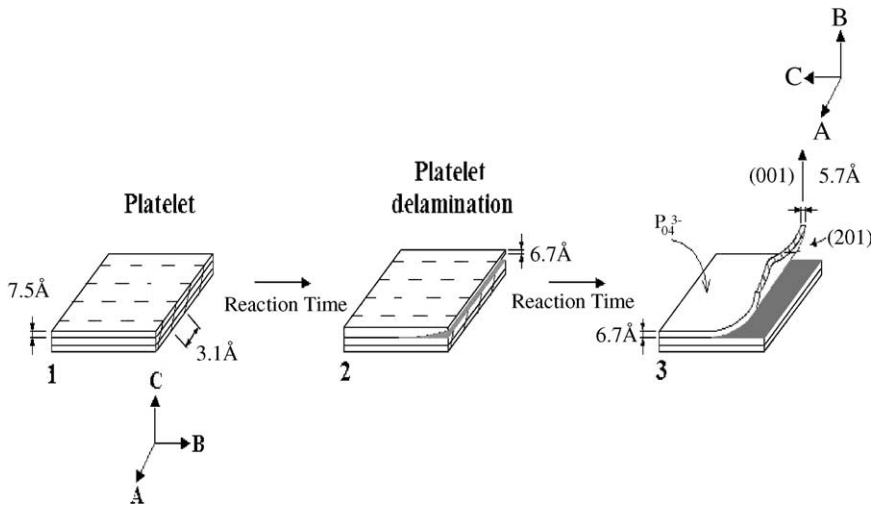

Fig. 6. Schematic representation of $VOHPO_4{\cdot}0.5H_2O$ crystallisation mechanism.

$VOHPO_4{\cdot}0.5H_2O$. We propose that the (0 0 1) and (2 0 1) planes of the hemihydrate grow out from the exposed $d = 7.5$–6.7 and 3.1 Å planes of the platelet, resulting in the familiar distorted rosette like morphology of $VOHPO_4{\cdot}0.5H_2O$, as shown schematically in Fig. 6.

According to this hypothesis, reduced, unreacted or undissolved vanadium oxide does not play an important role in this scheme, but its full dissolution proceeds rapidly helping to generate a high supersaturation when ortho-H_3PO_4 is added to the synthesis medium. This work defines for the first time the nucleation of $VOHPO_4{\cdot}0.5H_2O$ on the edges of $VOPO_4{\cdot}H_2O$ platelets and identifies the origin of the morphology of $VOHPO_4{\cdot}0.5H_2O$, which in turn determines the morphology of $(VO)_2P_2O_7$, the major phase present in VPO catalysts for *n*-butane oxidation.

4. Conclusion

In situ X-ray diffraction during the synthesis of $VOHPO_4{\cdot}0.5H_2O$ allowed the detection of the delaminated edges of $VOPO_4{\cdot}H_2O$ as the nucleation point for the formation of $VOHPO_4{\cdot}0.5H_2O$ and identified a mechanism whereby the familiar rosette type morphology of $(VO)_2P_2O_7$ is generated.

Acknowledgements

The authors acknowledge financial support from the Materials and Surface Science Institute, University of Limerick, Limerick, Ireland. Leonard O'Mahony would like to thank the CLRC Daresbury Laboratory, UK, for beam time on Station 16.4 and Dr. David Talyor for his assistance with setting up the synthesis cell.

References

[1] G. Centi, Catal. Today 16 (1993) 173.
[2] V.V. Guliants, J.B. Benziger, S. Sundaresan, I.E. Wachs, J.M. Jehng, J.E. Roberts, Catal. Today 28 (1996) 275.
[3] J.R. Ebner, M.R. Thompson, Catal. Today 16 (1993) 51.
[4] G.J. Hutchings, A. Desmartin-Chomel, R. Olier, J.C. Volta, Nature 368 (1994) 41.
[5] G.J. Hutchings, A. Burrows, S. Sajip, C.J. Kiely, K.E. Bere, J.C. Volta, A. Tuel, M. Abon, Proceedings of the Third World Congress on Oxidation Catalysis, 1997, p. 209.
[6] G.J. Hutchings, C.J. Kiely, M.T. Sananes-Schulz, A. Burrows, J.C. Volta, Catal. Today 40 (1998) 273.
[7] H.S. Horowitz, C.M. Blackstone, A.W. Sleight, G. Teufer, Appl. Catal. 38 (1988) 193.
[8] D.J. Thompson, M.O. Fanning, B.K. Hodnett, J. Mol. Catal. A: Chem. 198 (2003) 125.
[9] G. Busca, G. Centi, F. Trifiro, V. Lorenzelli, J. Phys. Chem. 90 (1986) 1337.
[10] G. Busca, G. Centi, F. Trifiro, Appl. Catal. 25 (1986) 265.
[11] E. Bordes, Catal. Today 1 (1) (1987) 499.
[12] E. Bordes, Catal. Today 3 (1) (1988) 163.
[13] B.K. Hodnett, Heterogeneous Catalytic oxidation: Fundamentals and Technological Aspects of the Selective and Total Oxidation of Organic Compounds, Wiley, New York, 2000.
[14] B.K. Hodnett, Catal. Rev. Sci. Eng. 27 (1985) 373.
[15] B.C. Giessen, G.E. Gordon, Science 159 (1968) 973.
[16] P. Barnes, A.C. Jupe, S.L. Colston, S.D. Jacques, A. Grant, T. Rathbone, M. Miller, S.M. Clark, R.J. Cernik, Nucl. Instrum. Meth. Phys. Res. B 134 (1998) 310.
[17] S.M. Clark, R.J. Cernick, A. Grant, S. York, P.A. Atkinson, A. Gallagher, D.G. Stokes, S.R. Gregory, N. Harris, W. Smith, M. Hancock, M.C. Miller, K. Ackroyd, R. Farrow, R. Frances, Mater. Sci. Forum 228–231 (1996) 213.
[18] S.M. Clark, Nucl. Instrum. Meth. Phys. Res. A 381 (1996) 161.
[19] E. Bordes, P. Courtine, C.R. Acad. Sci. Paris 274C (1972) 1375.
[20] E. Bordes, P. Courtine, Ann. Chim. (Paris) 8 (1973) 105.
[21] E. Bordes, P. Courtine, J.W. Johnson, J. Solid State Chem. 55 (1984) 270.